Modulating the reactivity of chromone and its derivatives through encapsulation in a self-assembled phenylethynylenebis-urea host

ARTICLE *in* JOURNAL OF PHOTOCHEMISTRY AND PHOTOBIOLOGY A CHEMISTRY · SEPTEMBER 2015

Impact Factor: 2.5 · DOI: 10.1016/j.jphotochem.2015.09.003

Journal of Photochemistry and Photobiology A: Chemistry 315 (2016) 14–24

Contents lists available at ScienceDirect

Journal of Photochemistry and Photobiology A: Chemistry

journal homepage: www.elsevier.com/locate/jphotochem

Invited feature article

Modulating the reactivity of chromone and its derivatives through encapsulation in a self-assembled phenylethynylene *bis*-urea host

Sahan R. Salpage[a], Logan S. Donevant[a], Mark D. Smith[a], Andreas Bick[b], Linda S. Shimizu[a,*]

[a] Department of Chemistry and Biochemistry, University of South Carolina, Columbia, SC 29208, USA
[b] Scienomics SARL, 16 rue de l'Arcade, 75008 Paris, France

ARTICLE INFO

Article history:
Received 6 June 2015
Received in revised form 30 August 2015
Accepted 1 September 2015
Available online 4 September 2015

Keywords:
Chromones
Bis-urea macrocycles
[2+2] photocycloadditions
GCMC simulations

ABSTRACT

This manuscript reports on the modulation of the photoreactivity of a series of chromones, also known as benzo-γ-pyrones, by absorption into a porous self-assembled host formed from phenylethynylene *bis*-urea macrocycles. Chromone and four derivatives namely 6-fluorochromone, 6-bromochromone, 7-hydroxy-4-chromone, and 3-cyanochromone are unreactive in the solid-state. Each of these derivatives was loaded into the nanochannels of self-assembled phenylethynylene *bis*-urea macrocycles to form solid host·guest complexes, which were subsequently UV-irradiated at room temperature under argon atmosphere. We observed that chromone and 6-fluorochromone underwent selective [2+2] photodimerization reactions to produce *anti*-HT dimers in high selectivity and conversion. The 6-bromochromone also reacted in high selectivity and conversion to afford an aryl coupling adduct. In each case, the products were extracted, and the crystalline host recovered. In comparison, 7-hydroxy-4-chromone, and 3-cyanochromone were unreactive within the complex. Simple GCMC simulation studies suggest that chromone, 6-fluorochromone, and 6-bromochromone were loaded in orientations that facilitate photoreaction, and correctly predicted that the *anti*-HT dimer would be favored in the chromone case. In contrast, *syn*-HH dimers were predicted by GCMC simulations for the halogen containing derivatives but were not observed. The simulations with 7-hydroxy-4-chromone were in agreement with the observed reactivity. We compare these computational and experimental findings and suggest future methods for optimizing simulation parameters. Our goal is to expand the scope and accuracy of the simulations to be able to predict the reactivity of guests encapsulated within columnar nanotubes.

1. Introduction

Inspired by nature's exquisite control over reactivity within the defined spaces of enzyme active sites, chemists have designed and investigated many molecular and supramolecular hosts as well as examined the use of porous materials to facilitate the reaction of encapsulated guests [1–7]. These 'nanoreactors' provide confined environments to induce selectivity, modulate the reaction pathway, and potentially catalyze the reaction [8]. Our group studies how the photolysis of small organic molecules is altered and influenced by the encapsulation within the cylindrical channels of stable, porous, crystalline hosts [9]. These hosts are formed through the supramolecular assembly of *bis*-urea macrocycles, such as the phenylethynylene *bis*-urea **1**, which self-assembles into columns that contain guest accessible channels of ~0.9 nm diameter (Fig. 1). Here, we investigate the application of this host to uptake chromone and its derivatives and study the effects of this encapsulation on the subsequent photoreactions versus the reactions of these derivatives in their solid-state form. Specifically, this manuscript applies systematic experimental and computational methods to evaluate: (1) the reactivity of chromone and four of its derivatives in the solid-state; (2) the use of GCMC simulations to investigate the organization of guests within the confined channel of a self-assembled phenylethynylene *bis*-urea host and to analyze if neighboring guests are aligned for facile photoreaction; and to evaluate experimentally (3) the uptake of chromones and their subsequent reactivity upon UV-irradiation.

Chromone (4H-1-benzopyran-4-one) belongs to the flavonoid family. Flavonoids play a vital role in plants as secondary metabolites [10]. Chromone serves as a key scaffold in synthetic organic chemistry [11], medicinal chemistry [12], and drug discovery [13]. In solution, simple chromones may undergo photodimerizations and photoaddition reactions [14] with olefins and acetylenes. For example, benzene solution UV-irradiation of

* Corresponding author.
E-mail address: shimizls@mailbox.sc.edu (L.S. Shimizu).

http://dx.doi.org/10.1016/j.jphotochem.2015.09.003
1010-6030/

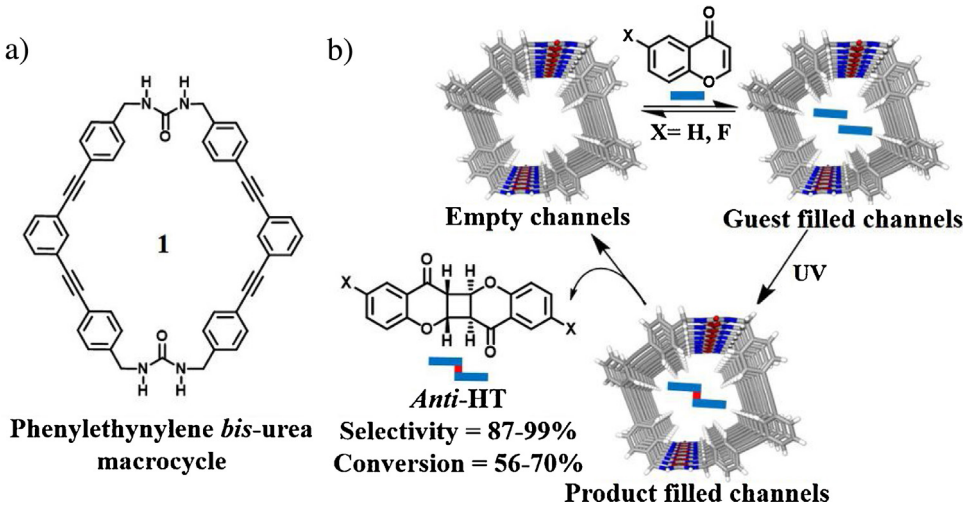

Fig. 1. Self-assembled phenylethynylene *bis*-urea macrocycles used as a confinement for conducting selective photodimerization of chromones. (a) Structure of the phenylethynylene *bis*-urea macrocycle [21]. (b) Loading of chromone and 6-fluorochromone affords host **1**·guest complexes that facilitated the selective formation of the respective *anti*-HT photodimers upon UV-irradiation.

chromone produced *anti*-HT and *trans-fused* HT dimers in ~1:1 ratio with 30% conversion and 99% yield [15]. The dimerization efficiency greatly depended upon the concentration of chromone [16]. Indeed, UV-irradiation of chromone-2-carboxylic esters (methyl, ethyl, or *iso*-propyl) in acetonitrile solutions produced *anti*-HH dimers from the triplet excited state while solid state reactions of methyl and *iso*-propyl chromone-2-carboxylic ester yielded the *anti*-HT dimers, and no solid state reaction was observed in ethyl derivative or for the parent chromone. Hanifin and Cohen reported the photoreactions of chromone with tetramethylethylene, 1-dimethoxyethylene, cyclopentene, and 2-butyne to obtain a variety of cycloadducts [17,18]. Nath et al. employed the photocycloaddition reaction of 2, 3, 7-trimethylchromone with ethylene as a key reaction in the synthesis of two marine natural products [19]. Studies from Valiulin and Kutateladze showed that the Diels–Alder adducts of chromones could undergo an intramolecular [2π+2π] alkene–arene photocyclization reaction [20].

Herein, we examine the utility of host **1** to bind, organize and facilitate the photoreactions of a series of simple chromones in the solid-state. Host **1** is formed by the columnar self-assembly of a phenylethynylene *bis*-urea macrocycle (Fig. 1a) [21]. This assembly process is driven by the urea hydrogen-bonding motif as the compound crystallized from DMSO. Heating drives off the DMSO solvent leaving open columnar channels, which are accessible to new guests. Our study into the utility of this host proceeded through both experimental investigation of what guests can be loaded into this confined channel as well as through GCMC simulations to predict not only guest absorption but also subsequent effects of this confinement on guest reactivity. The GCMC simulations were carried out using Monte Carlo for Complex Chemical Systems (MCCCS) Towhee [22] plug-in built into Scienomics' Materials Processes and Simulations (MAPS) platform [23] and suggested that the chromone, 6-fluorochromone, 6-bromochromone, and 7-hydroxy-4-chromone would load into the channels of host **1**; however, simulations predict that only the first three compounds would be favorably positioned for photoreactions. Simulations were not carried out on 3-cyanochromone due to incompatibility of the configurational bias settings with the cyano functional group and consistency of the bias settings with previous simulations.

The simulations suggest that the orientation of chromone inside the channel should favor formation of *anti*-HT photodimers. In comparison, the *syn*-HH dimers were predicted for 6-fluorochromone, and 6-bromochromone. Experimentally, we confirmed that the crystalline chromones were unreactive and stable to prolonged UV-irradiation. Host **1** absorbed each of these guests from solution to form solid-state host·guest complexes with the host:guest binding ratios dependent on the size and polarity of the guests (Fig. 1b). We tested if the solid-state photochemistry of chromones was modulated by incarceration within the crystalline host. Upon UV-irradiation of the respective host **1**·guest complexes, both chromone and 6-fluorochromone underwent [2+2] photodimerization reactions within the host in high conversion and selectivity. We observed 70% of chromone and 56% of 6-fluorochromone converted into photodimers. The *anti*-HT dimers were afforded as the major products in these host·guest complexes with 87% selectivity for chromone and >99% for 6-fluorochromone. The 6-bromochromone also reacted within the host complex forming a coupling adduct in high selectivity (>99%) and 70 % conversion. In this case, no [2+2] photocycloaddition was observed. In comparison, 7-hydroxy-4-chromone, and 3-cyanochromone proved to be unreactive within the host·guest complexes. The GCMC simulations predicted the reactivity of chromone, 6-fluorochromone, 6-bromochromone, and 7-hydroxy-4-chromone when encapsulated within the host. However, calculations predicted the observed product selectivity only in the case of chromone, which contains no additional polar functional groups. Our future goals are to synergistically evaluate the reactivity of encapsulated guests while concurrently optimizing GCMC simulations. We are currently addressing the computational simulations by evaluating new force fields, probing the effects of configurational bias settings, and testing variety of MC moves as well as probabilities.

2. Experimental

2.1. Materials and methods

All chemicals were purchased from Aldrich or VWR. Chromone and all its derivatives were further purified by recrystallization prior to loading. The phenylethynylene *bis*-urea macrocycle was prepared and recrystallized from DMSO to obtain host **1**·DMSO according to previous procedures [21]. Thermogravimetric analysis (TGA) was carried out in TA instrument SDT-Q600 to evacuate DMSO solvent from the channels of host **1**·DMSO prior to loading

studies. UV–vis data was collected on SoftMax M2e spectrophotometer. ^{1}H NMR and ^{13}C NMR spectra were recorded on Varian Mercury/VX 300 and VX 400 NMR. The X-ray intensity data were collected at 100(2) K using a Bruker SMART APEX diffractometer (Mo Kα radiation, λ = 0.71073 Å) [24]. The raw area detector data frames were reduced and corrected for absorption effects using the SAINT+ and SADABS programs [24]. The structures were solved by direct methods with SHELXS [25]. Subsequent difference Fourier calculations and full-matrix least-squares refinement against *F*2 were performed with SHELXL-2014 [25] using OLEX2 [26]. All non-hydrogen atoms were refined with anisotropic displacement parameters. Hydrogen atoms were located in difference maps before being included as riding atoms with refined isotropic displacement parameters.

2.2. Crystallization of 7-hydroxy-4-chromone, and 3-cyanochromone

Each compound (50 mg) was added to a scintillation vial with 2 mL of acetonitrile and heated. Single crystals suitable for X-ray analysis were obtained upon cooling.

2.2.1. Loading of guest molecules and calculating the binding ratios

The solvent was removed from freshly recrystallized host **1**·DMSO by TGA or by heating samples (∼50 mg) at 120 °C 1 h. Next empty host **1** crystals (15 mg) were soaked in solutions containing the guest (1 mM). Loading studies of chromone, 6-fluorochromone, and 6-bromochromone were carried out in hexane at 45 °C, while 7-hydroxy-4-chromone and 3-cyanochromone were carried out at rt in acetonitrile. The uptake of the guests into the host **1** was monitored through the change in the absorbance of the solution over time (from 0 to 3 h). A standard Beer–Lambert curve was generated for each guest and used to calculate the binding ratios (see Figs. S6–S10, SI).

2.2.2. UV-irradiation of chromones

Recrystallized samples of chromones (10 mg) were placed in Norell S-5-500-7 NMR tubes (with 100% transmittance up to 400 nm) and purged with argon. Each sample was UV-irradiated for 96 h at 26 °C. Samples were dissolved in $CDCl_3$ (0.6 mL) or CD_3CN (0.6 mL) and analyzed by ^{1}H NMR.

2.2.3. UV-irradiation of host 1·guest complexes

All photoreactions were performed in Norell S-5-500-7 NMR tubes using 15 mg of each complex under argon atmosphere. Each sample was UV-irradiated using a Hanovia 450 W medium pressure mercury arc lamp cooled in a quartz immersion well. The irradiation chamber temperature was kept at 26 °C. Samples (15 mg) were removed periodically (0, 3, 12, 24, and 96 h), extracted into $CDCl_3$ (0.6 mL) via ultrasonic sonication (15 min), and monitored by ^{1}H NMR. The filtrate with the photoproducts and the unreacted starting materials was decanted from the solid the host. The host was recovered, dried, and reused. Conversion of the starting materials to products was calculated using the ratio of integrals between starting material and corresponding product.

2.2.4. Crystallization of chromone and 6-fluorochromone photolysis products

At the end of the photoreactions, the encapsulated guests were removed from the host by extraction with $CHCl_3$. Products were separated from residual starting materials by preparative TLC. The crystals of chromone photodimers, both *anti*-HT and *anti*-HH, were obtained through slow evaporation of the dimer mixture in $CDCl_3$ (∼10 mg/mL). Crystals of 6-fluorochromone *anti*-HT photodimer were obtained by slow evaporation of dimer solution in $CDCl_3$ (∼10 mg/mL).

2.2.5. Grand Canonical Monte Carlo (GCMC) simulations

All GCMC simulations were performed using the Monte Carlo for Complex Chemical Systems (MCCCS) Towhee plug-in built into Scienomics' Materials Processes and Simulations (MAPS) platform [23] as previously reported [27]. Each guest was built using the amorphous builder within MAPS and their chemical potentials were calculated on a systems containing 100 guest molecules via a 5×10^4 step canonical MC simulation with MCCS Towhee and using the Widom insertion method and the Dreiding force field [28]. Next, a periodic simulation cell was constructed by importing the atomic coordinates from the X-ray structure of host **1**·nitrobenzene into MAPS. The nitrobenzene guests were removed from this structure. New host **1**·guest complexes were generated using the calculated guest chemical potential values. Finally, GCMC simulations were performed using Martin and Frischknecht configurational bias setting [29] for 1×10^6 steps, where the chemical potential (μ) of the corresponding guest was kept constant and the system was maintained at standard ambient constant temperature (*T*, 298.15 K) and constant volume (*V*). The Martin and Frischknecht configurational bias setting was used in the GCMC simulations for all chromone derivatives, however that scheme was incapable of setting up the simulations for the cyano derivative. Therefore, no simulations were performed for the cyano derivative.

3. Results and discussion

Macrocycle **1** self-assembled from DMSO to afford crystals with columnar channels. Initially, these channels are filled with disordered solvent but heating (120 °C) removes the DMSO to afford accessible channels, which can be filled with new guests (Fig. 3a). Previous work demonstrated that the ∼0.9 nm diameter nanochannels of the self-assembled phenylethynylene *bis*-urea host are accessible to gases including Xe and CO_2 [27,30]. The channels can also accommodate a range of organic guests including coumarins, acenaphthylene and stilbenes [21,27]. Confinement of guests within the nanochannels of host **1** facilitated the selective [2 + 2] photodimerization reactions of coumarin, 6-methyl coumarin, 7-methyl coumarin and acenaphthylene in good conversion. In comparison, stilbenes and 7-methoxy coumarin were unreactive. We turned to GCMC simulations to probe the origin of these changes in reactivity and selectivity, which afforded good predictions for these simple aromatic guests [27]. Here, we test utility and scope of the previously employed GCMC simulation protocol to predict if chromone and its derivatives (1) will be absorbed by this host and (2) will be reactive inside the confined space of the host. These chromones provide a challenging test of our methodology because they are relatively less reactive than the simple coumarins. They also present a range of polar substituents (hydroxyl, fluoro, bromo, or cyano), which introduce additional intermolecular interactions between neighboring guests as well as between the guests and the channel walls. Thus, these chromones serve as challenging targets to assess the scope and utility of the computational simulations.

As our goal is to compare the effects of encapsulation on the solid-state reactivity of the chromone guests, we first set out to analyze the structures of chromone and its derivatives in the solid state and investigate their reactivity. Pioneering work from Schmidt and co-workers on crystalline cinnamic acid derivatives elucidated the effects of molecular packing and orientation of the reactants in the crystalline lattice and led to the 'topochemical postulates' [31–33]. These postulates enable prediction of the product conformation by analysis of the crystalline structures of the reactants. Photocycloadditions are generally favorable when the double bonds of the reacting monomers are within 4.2 Å and aligned in parallel [34]. Although relatively simple in structure,

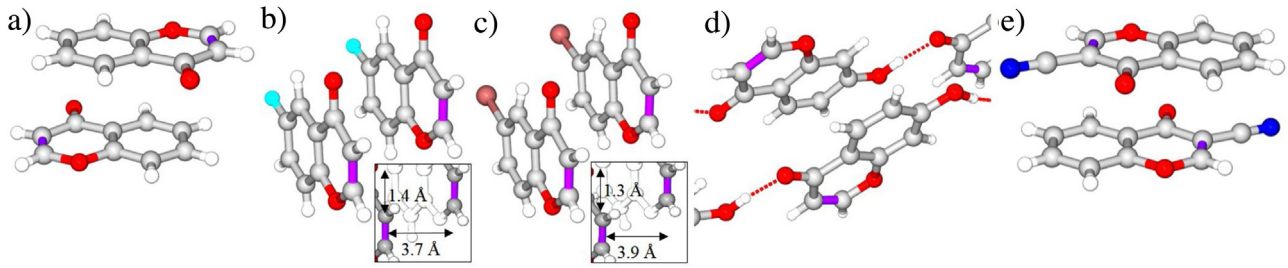

Fig. 2. Analysis of chromone solid-state structures highlights the closest contact between potentially reactive alkenes (purple bonds). (a) Pairing of chromones via aryl stacking interactions [36]. (b) View of close pairs of 6-fluorochromone (inset shows distance between reactive olefins) [36]. (c) Relative positioning of 6-bromochromone (inset shows distance between reactive olefins). (d) Hydrogen bonded chains of 7-hydroxy-4-chromone. (e) Relative positioning of 3-cyanochromone.

only 6-bromochromone had previously been reported in the Cambridge Crystallographic Database [35]. Thus, we sought to grow single crystals of these compounds suitable for X-ray diffraction studies. Crystals of chromone were obtained from a mixture of chloroform/hexanes [15,36] while crystals of 6-fluorochromone [36], 7-hydroxy-4-chromone and 3-cyanochromone were obtained by the cooling of hot acetonitrile solutions (25 mg/mL). Two new structures are reported here. Pale red plates of 7-hydroxy-4-chromone crystallized in monoclinic space group $P2_1/c$. Colorless parallelogram-shaped plate crystals of 3-cyanochromone crystallized triclinic space group $\bar{P}$.

Fig. 2 shows the arrangement of the reactive alkenes in chromone and in each of the four derivatives. Comparison of these structures shows that they exhibit markedly different relative orientations and distances between the potentially reactive alkenes. In the structure of chromone itself, the neighboring chromone molecules are paired through face-to-face aryl stacking interactions (3.63 Å ring centroid to centroid) with the electron rich portion of one chromone situated over the electron poor portion of its neighbor, which minimizes dipole interactions (Fig. 2a). This places the reactive olefins far apart from each other (closest C—C distance = 6.7 Å) disfavoring subsequent [2 + 2] cycloaddition in the solid state. Similar pairing is observed for 3-cyanochromone (Fig. 2e), which are stabilized by aryl stacking interactions (ring centroid–centroid distance = 3.5 Å) and by CH—N and CH—O hydrogen bonding. Here, the electron withdrawing cyano group is positioned under the electron rich aryl group of the neighboring molecule. This positions the reactive alkenes on opposite sides, disfavoring subsequent reaction (closest C—C distance = 6.6 Å). In the 7-hydroxy-4-chromone structure, strong OH—O hydrogen bonding dominates the crystal packing. Individual molecules are organized into one-dimensional chains through hydrogen bonds between the hydroxyl group on one molecule and the carbonyl oxygen of the neighboring molecule (Fig. 2d, O—O = 2.6 Å, <OHO = 168.5°). The chains stack into layers with offset aryl stacking interactions (3.3 Å) stabilizing the layers. (Fig. 2d and Supporting information Fig. S4). The reactive alkenes are preorganized far apart (closest C—C distance = 5.4 Å) again disfavoring photoreaction. In summary, analysis of the crystal structures led to the hypothesis that chromone, 7-hydroxy-4-chromone and 3-cyanochromone are poor substrates for solid-state photolysis reactions.

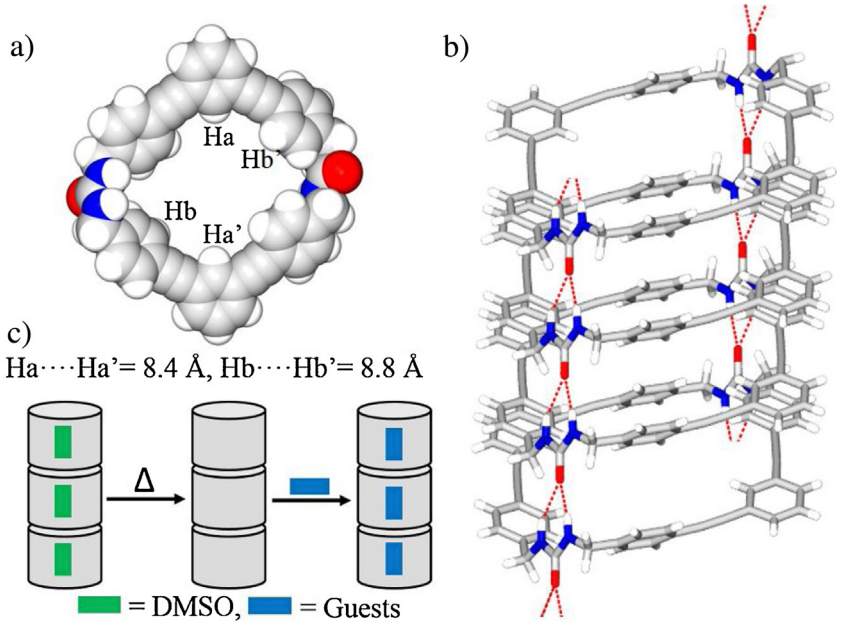

Fig. 3. Host **1** structure and schematic of guest exchange. (a) Space filling model of host from X-ray structure of host **1**·nitrobenzene emphasizes its almost round channel with the dimensions Ha . . . Ha′ = 8.4 Å and Hb . . . Hb′ = 8.8 Å. (b) View down a single column organized through the urea hydrogen bonding motif. (c) Schematic representation of crystals used for this study, which are readily obtained by recrystallization from DMSO. The solvent was removed by heating to obtain porous nanochannels that can be loaded with new guests.

The halogen derivatives show a different orientation for their aryl stacking interactions, which appears to be strongly influenced by the presence of the halides. The neighboring 6-fluorochromones interact through off-set aryl stacking interactions with a ring centroid–centroid distance of 3.7 Å (Fig. 2b). However, the enone sides of neighboring chromones are aligned on the same side and their halides are oriented in similar directions. The potentially reactive alkenes are close (bond centroid–centroid distance = 3.7 Å) and slightly offset by 1.6 Å. Similar molecular arrangement was observed in 6-bromochromone with offset π-stacking interactions (3.9 Å) placing the reactive olefins close in space 3.9 Å and offset by 1.3 Å (Fig. 2c). Potentially, a favorable [2 + 2] photoreaction would favor *syn*-HH dimers.

Survey of the solid-state structures predicted that only 6-fluorochromone and 6-bromochromone are aligned for potentially [2 + 2] photodimerization reaction. Thus, we next tested the reactivity of the crystalline chromones. Samples of the each of the five recrystallized solids (10 mg) were UV-irradiated under argon for 96 h. Then the solids were dissolved and analyzed by ^{1}H NMR. Only resonances corresponding to the starting materials were observed (Fig. S5, SI), demonstrating that the photoreactions of these chromones are indeed unfavorable in the reported crystal forms.

Next, we sought to computationally predict if host **1** could be used to modulate the reactivity of these molecules. Fig. 3 illustrates the columnar structure of the assembled phenylethynylene *bis*-urea macrocycle, which is organized through the urea hydrogen bonding motif with (N)H . . . O hydrogen bond distances ranging from 2.06 to 2.20 Å [21]. The interior cross-section of the channel is almost round with dimensions of ∼8.4 Å × ∼8.8 Å. In addition to the bifurcated urea–urea hydrogen bonding, the columnar structure is further stabilized by edge to face aryl stacking and alkyne–π interactions. These crystal structure parameters were imported into the MAPS program and the coordinates for the

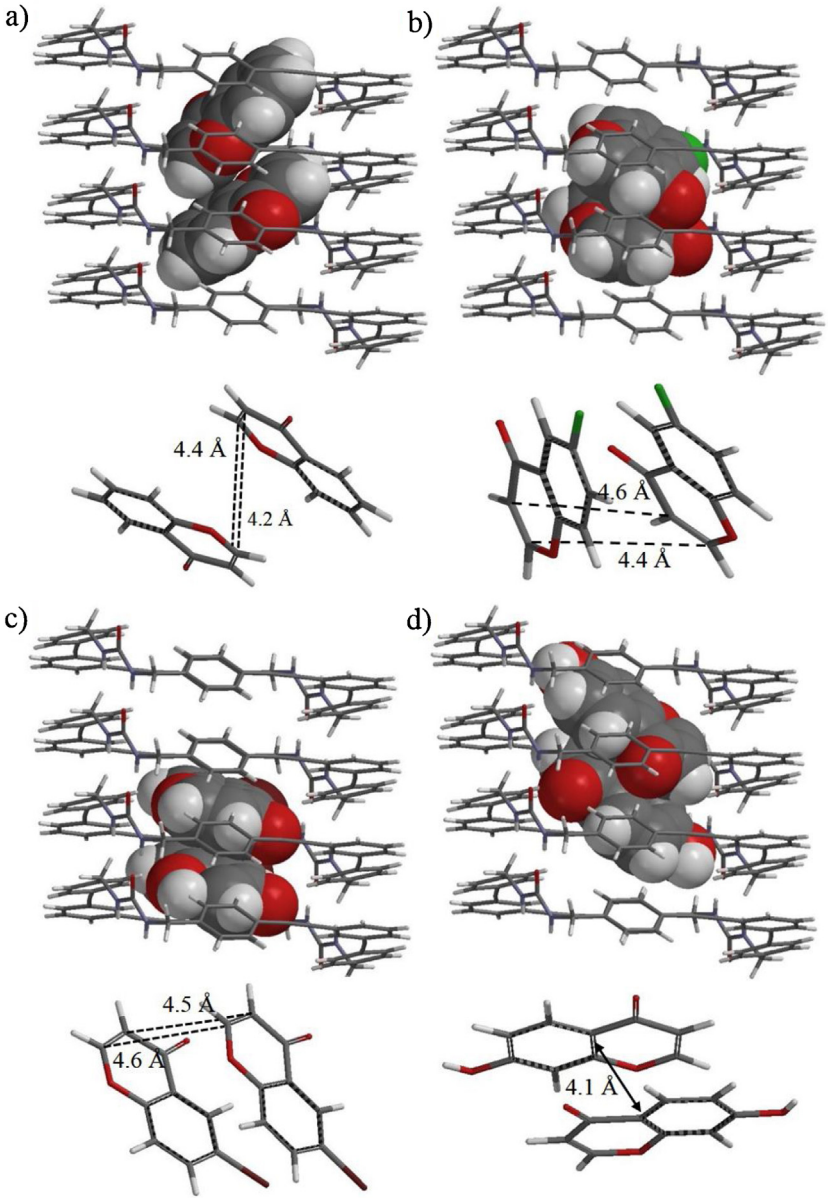

Fig. 4. Results of GCMC modeling of host **1**·guest complexes and analysis of the relative orientation of neighboring reactants. (a) Orientation and distance of neighboring chromones encapsulated in host **1** suggests *anti*-HT dimer will be favored. (b) Orientation and distance of neighboring 6-fluorochromones suggests *syn*-HH photodimer formation. (c) Orientation and distance of neighboring 6-bromochromones within host **1** suggests *syn*-HH dimer formation. (d) Orientation and distance of neighboring 7-hydroxy-4-chromones within host **1** appears to be unfavorable for [2+2] cycloadditions. (Centroid to centroid distance highlighted).

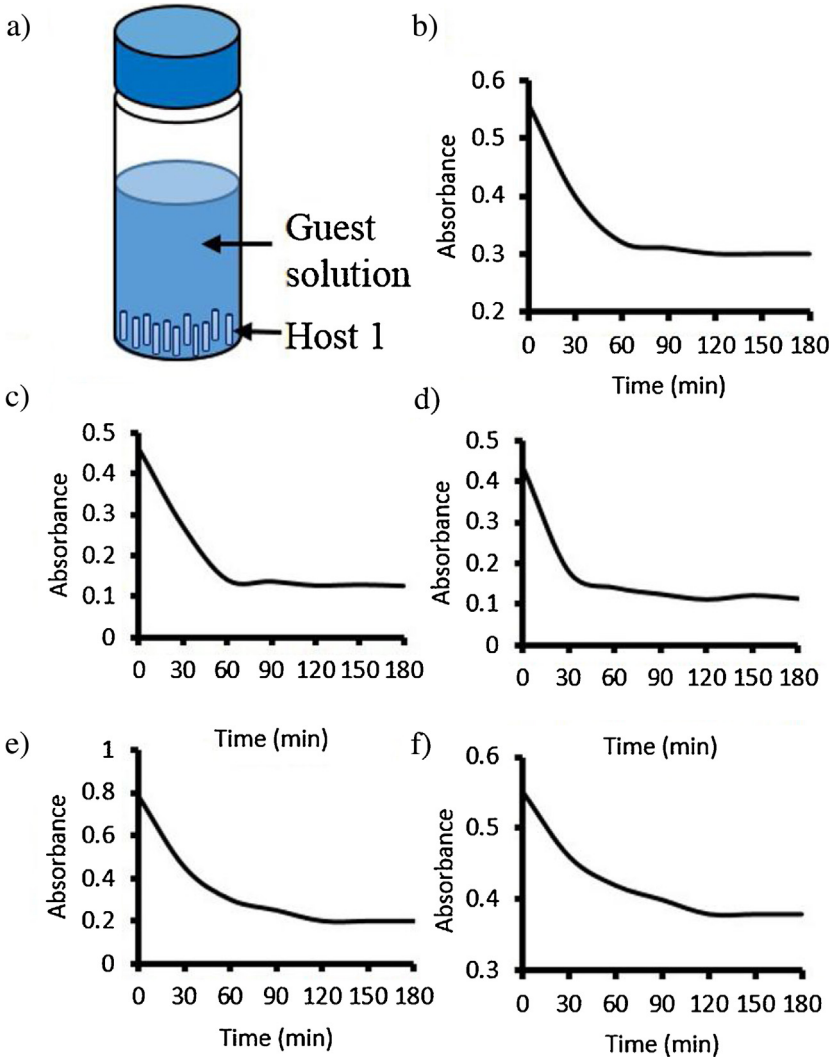

Fig. 5. Loading of the guests and the depletion of each guest from the solution monitored by UV/vis spectrophotometry. (a) Soaking of host **1** crystals in guest solutions. (b) Depletion of chromone from the solution (1 mM in hexanes at 45 °C) monitored at 290 nm, (c) depletion of 6-fluorochromone (1 mM in hexanes at 45 °C) monitored at 300 nm, (d) depletion of 6-bromochromone (1 mM in hexanes at 45 °C) monitored at 300 nm, (e) depletion of 7-hydroxy-4-chromone (1 mM in acetonitrile at rt) monitored at 295 nm, and (f) depletion of 3-cyanochromone (1 mM in acetonitrile at rt) monitored at 295 nm.

nitrobenzene guests were removed. The chemical potentials (μ) of the guests were calculated as previously described [27]. Next, 1×10^6 step Grand Canonical (μVT) Monte Carlo simulations were conducted for each guest using the Dreiding force field with predetermined guest chemical potentials (μ). We then analyzed the significant configurations of these GCMC simulations to investigate the fit of chromones within the nanochannels and to analyze if their relative orientation with respect to neighboring guests would be favorable for a photoreaction. Four of the five chromones were amenable to this simulation protocol. The cyano-derivative gave an error with the Martin and Frischknecht configurational bias setting [29]. We are currently examining the simulations of this molecule using different bias settings including Martin and Thompson [37].

During the simulation, two chromone molecules entered the channel and paired in the center of the host **1** (Fig. 4a). The primary stabilizing interactions are edge to face aryl stacking interactions. The distance between the aryl H of the channel wall and the benzene of the chromone molecules is ~2.6 Å. Of particular interest is the distance and orientation of the two potentially reactive alkenes. Here, the distances range between 4.2 and 4.4 Å, likely favorable for reaction. The two molecules are oriented to place the reactive olefins in an *anti*-fashion (Fig. 4a), suggesting a high probability to afford *anti*-HT photodimer upon UV-irradiation.

The structure of host **1**·6-fluorochromone was modeled using the same GCMC simulation procedure. The minimized structure is illustrated in Fig. 4b. The simulation suggests that the four molecules are arrange in pairs within the channels. Only the central pair is depicted in the figure for clarity. The molecules are stabilized by the edge to face pi interactions between aryl C—H

Table 1
Guests absorbed by host **1**.

Guest	Volume[a] (Å^3)	Polarity (D)	H:G
Chromone	127.84	3.54[b]	1:0.68
6-Fluoro chromone	133.28	4.23[a]	1:0.97
6-Bromo chromone	147.15	4.14[a]	1:0.97
7-Hydroxy-4-chromone	135.87	4.53[a]	1:1.07
3-Cyano chromone	144.97	7.16[a]	1:0.48

[a] Calculated in Spartan [38] using DFT (B3LYP) with 6-311++G** basis set.
[b] Ref. [39].

Table 2
Summary of photoreactions.

Guest	Entry	Host	Time (h)	Conv. (%)	Selectivity (%)				
					syn-HH	*syn*-HT	*anti*-HH	*anti*-HT	Coupling adduct
Chromone	1	–	96	0	–	–	–	–	–
	2	1	3	19	0	0	13	87	0
	3	1	12	46	0	0	13	87	0
	4	1	24	55	0	0	13	87	0
	5	1	96	70	0	0	13	87	0
6-Fluorochromone	6	–	96	0	–	–	–	–	–
	7	1	6	22	0	0	0	>99	0
	8	1	12	34	0	0	0	>99	0
	9	1	96	56	0	0	0	>99	0
6-Bromochromone	10	–	96	0	–	–	–	–	–
	11	1	3	25	0	0	0	0	>99
	12	1	6	52	0	0	0	0	>99
	13	1	24	70	0	0	0	0	>99
7-Hydroxy-4-chromone	14	–	96	0	–	–	–	–	–
	15	1	96	0	–	–	–	–	–
3-Cyanochromone	16	–	96	0	–	–	–	–	–
	17	1	96	0	–	–	–	–	–

from the channel wall and pi surface of the benzene moiety in 6-fluorochromone with a distance of 3.2 Å. The reactive olefins are aligned and separated by 4.4–4.6 Å, slightly longer than the 4.2 Å predicted for optimal reaction. We observed a similar packing and orientation of the molecules in the host **1**·6-bromochromone GCMC simulation (Fig. 4c). The molecules were arranged in pairs in the channels and show stabilizing edge to face interactions between the aryl C—H from the channel wall and the pi surface of the chromones. We observed a distances ranging from 4.4 to 4.6 Å between reactive olefins. Should a [2 + 2] cycloaddition reaction

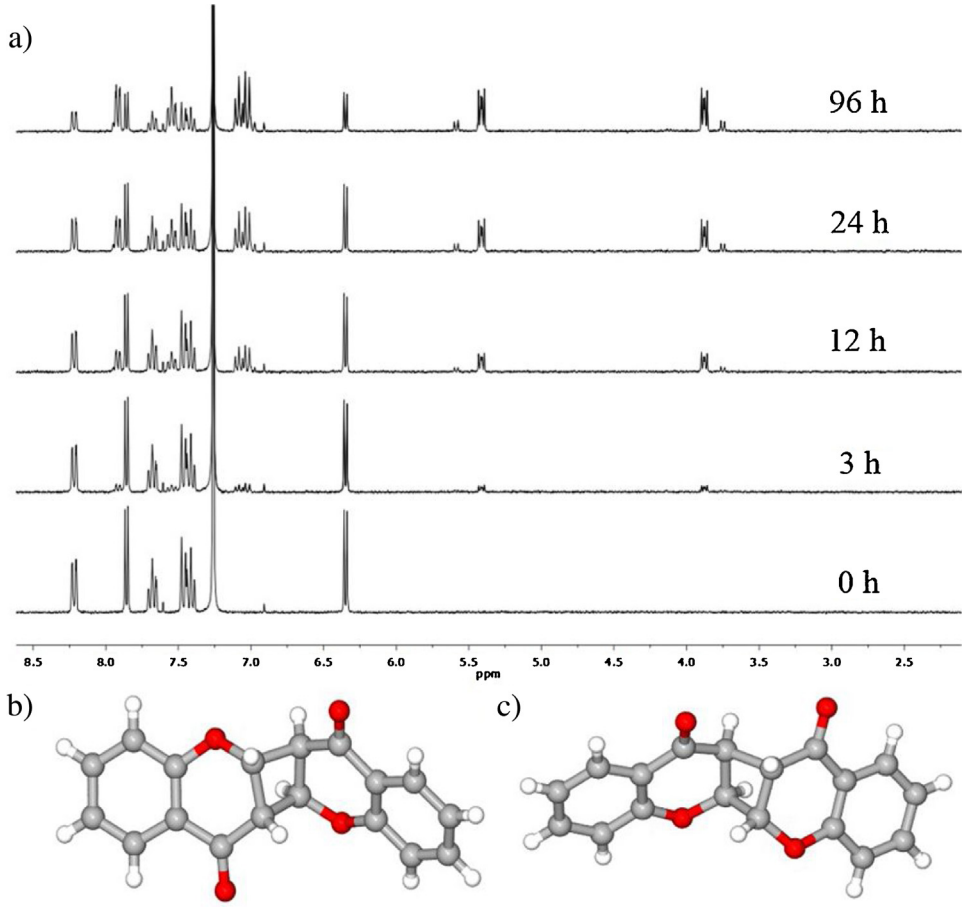

Fig. 6. Monitoring the photoreaction of host **1**·chromone and observed photoproducts. (a) ^{1}H NMR analysis of the photoreaction of host **1**·chromone in different time intervals. (b) Crystal structure of the *anti*-HT dimer, which was the major product. (c) Crystal structure of the *anti*-HH dimer.

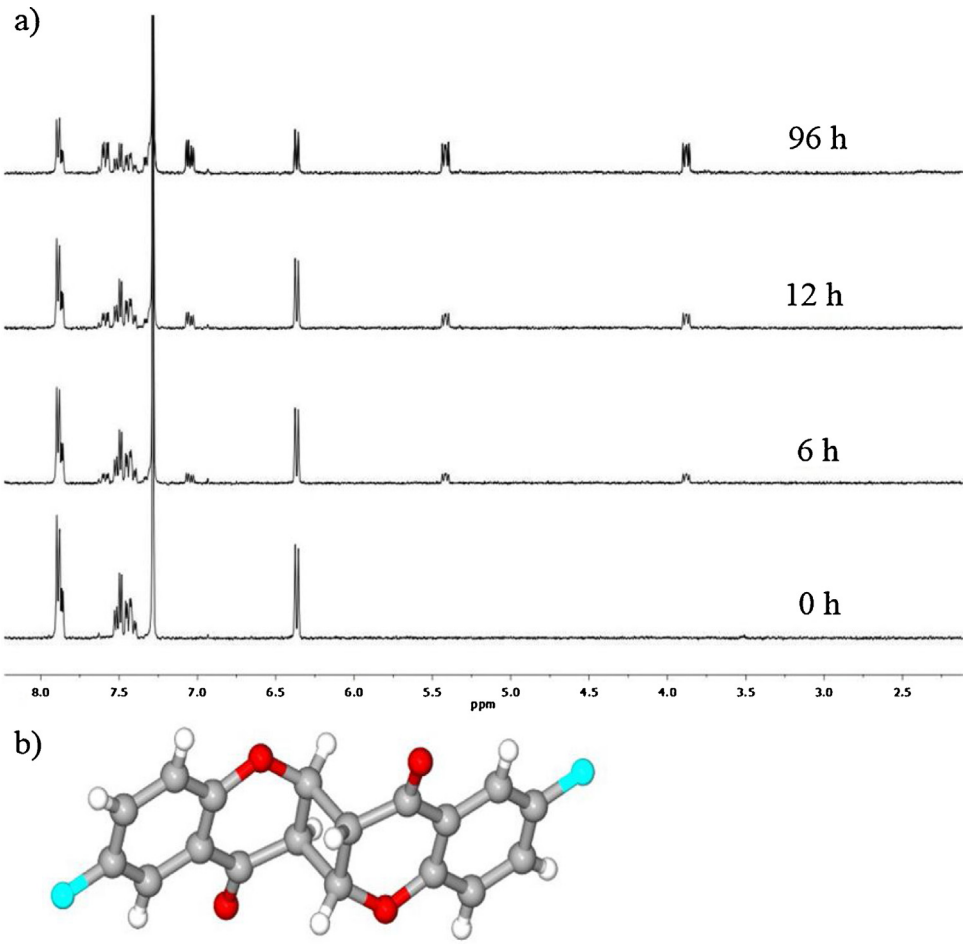

Fig. 7. Monitoring the photoreaction of host **1**·6-fluorochromone. (a) ^{1}H NMR analysis of the photoreaction of host **1**·6-fluorochromone in different time intervals. (b) Crystal structure of the *anti*-HT photodimer.

occur in these complexes upon UV-irradiation, we predict that both **1**·6-fluorochromone and host **1**·6-bromochromone would favor the formation of their respective *syn*-HH dimers.

A different relative orientation was observed for the guests within the simulated host **1**·7-hydroxy-4-chromone structure (Fig. 4d). Here, molecules are paired through offset aryl stacking interactions with the distance of 4.1 Å. There are no hydrogen bonding interactions apparent, suggesting that our force field and/or our protocol needs further optimization. The reactive olefins are far apart and unfavorably oriented for photoreaction. In summary, our GCMC simulations suggest that three of the four chromones tested may potentially undergo photochemical reactions and predicts that chromone should favor *anti*-HT products while the 6-fluorochromone and 6-bromochromone favor the formation of *syn*-HH photoproducts.

Next, the series of chromone derivatives were loaded into host **1**. First, the solvent was removed from freshly recrystallized host **1**·DMSO by heating and the empty crystals were equilibrated with 1 mM solutions of the guest (Fig. 4a). A UV–vis spectrophotometer was used to monitor the depletion of the guest from solution, and the host:guest binding ratios were calculated through comparison to standard Lambert–Beer plots with known concentrations of guests (see SI). For example, host **1** (15 mg) was soaked in a solution of chromone (1 mM in hexanes) at 45 °C for 0–3 h. The depletion of chromone from solution was monitored by absorbance spectroscopy at 290 nm (Fig. 5b). The absorbance reached a plateau by 2 h, suggesting that an equilibrium had been reached. Assuming that the loss of guest from solution is due to the absorption of the guest by host **1**, we calculated a host guest ratio of 1:0.68 by comparison of the final absorbance to a Lambert–Beer plot of known concentration of chromone in (hexanes). The binding ratios reported in Table 1 are the average ratio of three separate loading experiments.

From Table 1, it is apparent that all the derivatives tested could be loaded into host **1**; however, the loading ratio was not simply based on size. Indeed chromone (volume = 127.84 Å^3, polarity = 3.5 D), the smallest compound tested, showed a slightly lower binding ratio with 1:0.68 host **1**:chromone versus the larger and slightly more polar halide containing derivatives (polarity ~4.1 D), which loaded at 1:0.97. The more polar 7-hydroxy-4-chromone (4.5 D) showed a slightly higher ratio of 1:1.07. A relatively low binding ratio (1:0.48) was observed for the most polar 3-cyanochromone (7.16 D), which is similar in volume to 6-bromochromone, suggesting that shape likely also influences the binding ratio in addition to size and polarity.

To test the photoreactivity of these host·guest complexes samples (15 mg) were UV-irradiated at room temperature (26 °C) under an argon atmosphere using a Hanovia 450 W medium pressure mercury arc lamp. Samples (15 mg) were removed periodically (0, 3, 12, 24, and 96 h), extracted into $CDCl_3$ (0.6 mL). The photoproducts were monitored by ^{1}H NMR. Samples were also completely dissolved in DMSO-d6 to confirm that the guests could be completely removed from the crystals.

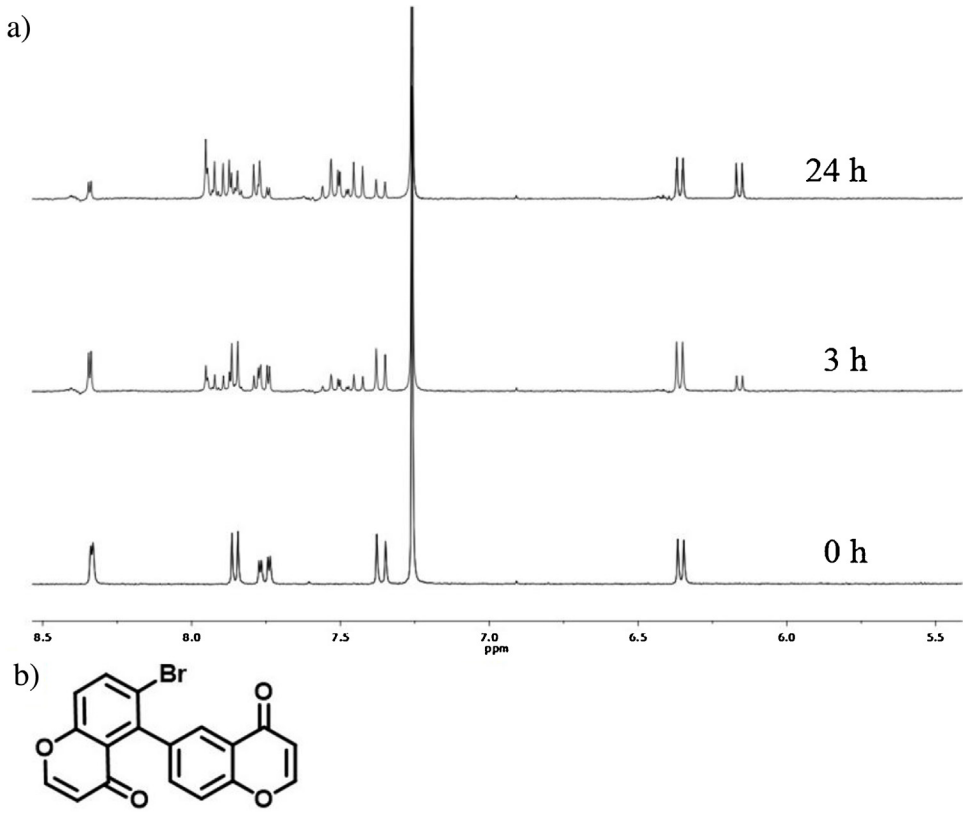

Fig. 8. Photoreaction of host **1**·6-bromochromone and observed photoproduct. (a) ^{1}H NMR analysis of the photoreaction of host **1**·6-bromochromone in different time intervals. (b) Structure of the coupling product.

Table 2 summarizes these photochemical studies and shows that three of the five encapsulated guests underwent photolysis reactions. After UV-irradiation of host **1**·chromone for 3 h, we observed 19% conversion of chromone to afford two photodimers (Table 2, entry 2). The ^{1}H NMR resonances for the major product, matched those reported for the *anti*-HT photodimer [15]. GC/MS was used to further monitor the selectivity and showed an *anti*-HT selectivity of 87.4% with the minor photodimer formed in 12.6% selectivity (see SI for GC/MS trace). Increasing the UV-irradiation time (12 h, entry 3; 24 h, entry 4, and 96 h, entry 5) gave an increase in conversion of chromone from 46% at 12 h to 70% at 96 h with similar selectivity for two photodimers (Fig. 6a). We were able to isolate the photoproducts using preparative TLC and single crystals suitable for XRD analysis of both photodimers were obtained from the slow evaporation of $CDCl_3$ solution. The two photodimers formed crystals with distinct morphology, allowing ready separation of both dimer products. Indeed, the structure of the major product, which formed as large colorless blocky crystals, was confirmed as the *anti*-HT (Fig. 6b). The minor photodimer, which formed thin colorless plates, was identified as the *anti*-HH dimer (Fig. 6c) and is the first report of the synthesis and characterization of this photodimer. In solution, chromone photodimerization was reported to yield two products, the *anti*-HT and the *trans*-fused HT photodimers in a maximum of 40% conversion [15]. The conversion was limited due to the higher absorption of the photodimers as compared with the starting chromone. [15] In contrast, in the host **1**·chromone solid complex the conversion of chromone to photodimers is enhanced to 70% and no *trans*-fused HT dimers were observed.

Similar UV-irradiation of the host **1**·6-fluorochromone crystals facilitated a remarkably selective photodimerization, yielding the *anti*-HT dimer with >99% selectivity in 22% conversion after 6 h (Table 2, entry 7). Fig. 7a shows new resonance for the *anti*-HT photodimer. Again, increasing the UV-irradiation time to 12 h or 96 h afforded increased conversion to 34% and 56% respectively with similarly high selectivity (entries 8 and 9). This is the first report of a [2 + 2]-photocycloaddition of 6-fluorochromone, and its structure was confirmed by X-ray diffraction.

We found that host **1**·6-bromochromone showed distinctly different reactivity inside host **1**. UV-irradiation of host **1**·6-bromochromone facilitated 25% conversion of the bromochromone to a single new product after 3 h (Table 2, entry 11). Inspection of the ^{1}H NMR showed alkenes resonances at 6.16 ppm (Fig. 8a) and that surprisingly no resonances were observed in the cyclobutane region (5.75–2.75 ppm) typical for [2 + 2] cycloadditions. Increasing the UV-irradiation time to 6 h or 24 h resulted in increased production of this product in 52% and 70% conversion respectively (entries 12 and 13). Longer irradiation times (>24 h) did not show any additional conversion. The products were extracted with chloroform and the residual 6-bromochromone was removed by preparative TLC (see SI). The product was characterized by NMR (^{1}H, ^{13}C, 2 D COSY) and HRMS. The formation of this aryl coupling product may suggest a radical mechanism due to the labile Br atom at the 6 position (see Fig. S18, SI). Halogenated chromones including 6-bromo and 6-flouro derivatives have been used to synthesize a variety of isoflavone structural motifs through metal catalyzed cross coupling reactions. A palladium catalyzed direct cross coupling of 6-bromo and 6-flourochromones with quinones [40] and a rhodium catalyzed direct oxidative cross coupling of 6-bromochromone with alkenes have been reported [41].

We found that the host **1**·7-hydroxy-4-chromone was stable to prolonged UV-irradiation (96 h, entry 15). This was the same as

what was observed for solid 7-hydroxy-4 chromone. The host **1**·3-cyanochromone complex was also photostable and was reisolated after 96 h of UV-irradiation (entry 17). Solid 3-cyanochromone crystals were also unreactive under similar conditions.

We next compared our experimental findings with the GCMC predictions. As predicted each of our compounds were able to be loaded into the nanochannels of host **1**. The simulations further suggested that chromone, 6-fluorochromone and 6-bromochromone would be reactive while the 7-hydroxy-4-chromone would likely be unreactive within their respective host **1** complexes, although the host **1**·3-cyanochromone complex was not amenable to our simulation protocol. The selectivity of the host **1**·chromone reaction was successfully predicted by our GCMC simulations for chromone, which indeed formed the *anti*-HT photodimer as its major product. Unfortunately, our current GCMC protocol did not accurately predict the selectivity of the halogen containing derivatives. Future work will focus on the optimization of the force field parameters, GCMC bias settings, type of the Monte Carlo moves, and probabilities to enable more accurate simulations of guest reactivity and selectivity within our host complexes. For example, more detailed force fields Amber_Cornell or CHARMM may increase the accuracy of the simulations. Our goal is to expand the scope and accuracy of our simulations in order to predict the reactivity of guests with different functionality.

4. Conclusions

In summary, a porous columnar host from self-assembled phenylethynylene *bis*-urea macrocycles was successfully employed to modulate the reactivity of chromone, 6-fluorochromone and 6-bromochromone, which were otherwise unreactive in the solid state. Encapsulated chromone and 6-fluorochromone underwent [2+2] photodimerization reactions to afford their respected *anti*-HT dimers in moderate to good yields with high selectivity. We observed 56–70% of reactants converted into photodimers and *anti*-HT dimers afforded in 87–99% selectivity. Chromone conversion to photodimers in the crystalline host complex (70% conversion) was remarkable when compared with prior reports from solution (40%) where conversion was thought to be limited by the stronger absorption of the photodimers versus the parent chromone [15]. This enhanced conversion suggests that encapsulation significantly stabilizes the products. For 6-fluorochromone, our studies gave the first reported formation of its *anti*-HT photodimer. In comparison, the photoreaction of encapsulated 6-bromochromone produced an unusual aryl coupling product in 70% conversion and >99% selectivity. Although bound by our host, 7-hydroxy-4-chromone and 3-cyanochromone were unreactive under UV-irradiation.

Our long term goal is to develop computational simulations to understand and to accurately predict the photoreactivity of a wide range of small organic reactants within the nanochannels of assembled hosts, which were readily recovered after extraction of the products. Thus far, our GCMC simulation gave mixed results with the compounds tested. The simulations correctly predicted that all these compounds could be loaded into the nanochannels of host **1**, but had only a 50% success rate of determining the product selectivity of the subsequent photoreactions. In particular, the reaction selectivity for encapsulated halogen containing derivatives (6-fluorochromone and 6-bromochromone) was incorrect. Current work focuses on exploring force fields that more accurately describe the non-bonded interactions and on the optimization of the GCMC bias settings.

Supporting information

X-ray crystal structures (CCDC 1402298-1402302) .cif files for 7-hydroxy-4-chromone, 3-cyanochromone, chromone *anti*-HT and *anti*-HH photodimers, 6-fluorochromone *anti*-HT photodimer, ^{1}H NMR and ^{13}C NMR spectra, loading data, Beer–Lambert plots, and simulation details.

Acknowledgement

This research was supported in part by the National Science Foundation (CHE-1305136)

Appendix A. Supplementary data

Supplementary data associated with this article can be found, in the online version, at http://dx.doi.org/10.1016/j.jphotochem.2015.09.003.

References

[1] V. Ramamurthy, S. Gupta, Supramolecular photochemistry: from molecular crystals to water-soluble capsules, Chem. Soc. Rev. 44 (2015) 119–135.
[2] P. Ballester, M. Fujita, J. Rebek, Molecular containers, Chem. Soc. Rev. 44 (2015) 392–393.
[3] D. Ajami, J. Rebek, More chemistry in small spaces, Acc. Chem. Res. 46 (2013) 990–999.
[4] V. Ramamurthy, J. Sivaguru, Controlling Photoreactions Through Noncovalent Interactions within Zeolite Nanocages, Supramolecular Photochemistry, John Wiley & Sons Inc., 2011, pp. 389–442.
[5] V. Ramamurthy, A. Parthasarathy, Chemistry in restricted spaces: select photodimerizations in cages, cavities, and capsules, Isr. J. Chem. 51 (2011) 817–829.
[6] Y. Inokuma, M. Kawano, M. Fujita, Crystalline molecular flasks, Nat. Chem. 3 (2011) 349–358.
[7] O.B. Berryman, H. Dube, J. Rebek, Photophysics applied to cavitands and capsules, Isr. J. Chem. 51 (2011) 700–709.
[8] V. Ramamurthy, B. Mondal, Supramolecular photochemistry concepts highlighted with select examples, J. Photochem. Photobiol. C Photochem. Rev. 23 (2015) 68–102.
[9] L.S. Shimizu, S.R. Salpage, A.A. Korous, Functional materials from self-assembled bis-urea macrocycles, Acc. Chem. Res. 47 (2014) 2116–2127.
[10] R. Verpoorte, J. Memelink, Engineering secondary metabolite production in plants, Curr. Opin. Biotechnol. 13 (2002) 181–187.
[11] J. Zhao, Y. Zhao, H. Fu, Transition-metal-free intramolecular Ullmann-type *O*-arylation: synthesis of chromone derivatives, Angew. Chem. Int. Ed. 50 (2011) 3769–3773.
[12] A. Gaspar, M.J. Matos, J. Garrido, E. Uriarte, F. Borges, Chromone: a valid scaffold in medicinal chemistry, Chem. Rev. 114 (2014) 4960–4992.
[13] R.S. Keri, S. Budagumpi, R.K. Pai, R.G. Balakrishna, Chromones as a privileged scaffold in drug discovery: a review, Eur. J. Med. Chem. 78 (2014) 340–374.
[14] M. Yusuf, I. Solanki, P. Jain, R. Kumar, Photochemical studies: chromones, bischromones and anthraquinone derivatives, Arabian J. Chem. (2015) , doi: http://dx.doi.org/10.1016/j.arabjc.2014.11.031 (in press).
[15] M. Sakamoto, M. Kanehiro, T. Mino, T. Fujita, Photodimerization of chromone, Chem. Commun. (2009) 2379–2380.
[16] M. Sakamoto, F. Yagishita, M. Kanehiro, Y. Kasashima, T. Mino, T. Fujita, Exclusive photodimerization reactions of chromone-2-carboxylic esters depending on reaction media, Org. Lett. 12 (2010) 4435–4437.
[17] J.W. Hanifin, E. Cohen, Photoaddition reactions of chromone, J. Am. Chem. Soc. 91 (1969) 4494–4499.
[18] J.W. Hanifin, E. Cohen, Photoaddition reactions of chromome, Tetrahedron Lett. 7 (1966) 5421–5426.
[19] A. Nath, A. Ghosh, R.V. Venkateswaran, Rapid, high-yield synthesis of the marine sesquiterpenes debromoaplysin and aplysin via the acid-catalyzed rearrangement of a cyclobutachromanol, J. Org. Chem. 57 (1992) 1467–1472.
[20] R.A. Valiulin, A.G. Kutateladze, First example of intramolecular [2π+2π] alkene–arene photocyclization in the chromone series and its synthetic utility, Tetrahedron Lett. 51 (2010) 3803–3806.
[21] S. Dawn, M.B. Dewal, D. Sobransingh, M.C. Paderes, A.C. Wibowo, M.D. Smith, J. A. Krause, P.J. Pellechia, L.S. Shimizu, Self-assembled phenylethynylene bis-urea macrocycles facilitate the selective photodimerization of coumarin, J. Am. Chem. Soc. 133 (2011) 7025–7032.
[22] M.G. Martin, MCCCS Towhee: a tool for Monte Carlo molecular simulation, Mol. Simul. 39 (2013) 1212–1222.

[23] Materials and Processes Simulations (MAPS), Copyright Scienomics SARL, Paris, France, 2004–2013.
[24] SMART, Version 5.631, SAINT+ Version 6.45a, Bruker analytical X-ray Systems, Inc., Madison, Wisconsin, USA, 2003.
[25] G. Sheldrick, A short history of SHELX, Acta Crystallogr. Sect. A 64 (2008) 112–122.
[26] O.V. Dolomanov, L.J. Bourhis, R.J. Gildea, J.A.K. Howard, H. Puschmann, OLEX2: a complete structure solution, refinement and analysis program, J. Appl. Crystallogr. 42 (2009) 339–341.
[27] S. Dawn, S.R. Salpage, B.A. Koscher, A. Bick, A.C. Wibowo, P.J. Pellechia, L.S. Shimizu, Applications of a bis-urea phenylethynylene self-assembled nanoreactor for [2 + 2] photodimerizations, J. Phys. Chem. A 118 (2014) 10563–10574.
[28] S.L. Mayo, B.D. Olafson, W.A. Goddard, DREIDING: a generic force field for molecular simulations, J. Phys. Chem. 94 (1990) 8897–8909.
[29] M.G. Martin, A.L. Frischknecht, Using arbitrary trial distributions to improve intramolecular sampling in configurational-bias Monte Carlo, Mol. Phys. 104 (2006) 2439–2456.
[30] C.R. Bowers, M. Dvoyashkin, S.R. Salpage, C. Akel, H. Bhase, M.F. Geer, L.S. Shimizu, Crystalline bis-urea nanochannel architectures tailored for single-file diffusion studies, ACS Nano 9 (2015) 6343–6353.
[31] G.M.J. Schmidt, Photodimerization in the solid state, Pure Appl. Chem. (1971) 647–678.
[32] M.D. Cohen, G.M.J. Schmidt, F.I. Sonntag, 384. Topochemistry. Part II. The photochemistry of trans-cinnamic acids, J. Chem. Soc. (1964) 2000–2013.
[33] M.D. Cohen, G.M.J. Schmidt, 383. Topochemistry. Part I. A survey, J. Chem. Soc. (1964) 1996–2000.
[34] K. Biradha, R. Santra, Crystal engineering of topochemical solid state reactions, Chem. Soc. Rev. 42 (2013) 950–967.
[35] R.J. Staples, W. Lea, Crystal structure of 6-bromochromone, C9H5BrO2, Z. Kristallogr. – New Cryst. Struct. (2005) 371–372.
[36] S.R. Salpage, M.D. Smith, L.S. Shimizu, Crystal structures and Hirshfeld surface analyses of 6-substituted chromones, CrystEngComm. (2015) Submitted manuscript ID: CE-ART-08-2015-001638.
[37] M.G. Martin, A.P. Thompson, Industrial property prediction using Towhee and LAMMPS, Fluid Phase Equilib. 217 (2004) 105–110.
[38] Spartan 10, Program for Calculation of Molecular Properties, Wavefunction Inc., Irvine, CA, USA, 2015.
[39] V.D. Orlov, I.A. Borovoi, V.N. Tishchenko, V.F. Lavrushin, Polarity of chromone and flavone molecules, Theor. Exp. Chem. 10 (1975) 73–75.
[40] Y. Moon, S. Hong, A facile route to isoflavone quinones via the direct cross-coupling of chromones and quinones, Chem. Commun. 48 (2012) 7191–7193.
[41] R. Samanta, R. Narayan, A.P. Antonchick, Rhodium(III)-catalyzed direct oxidative cross coupling at the C5 Position of chromones with alkenes, Org. Lett. 14 (2012) 6108–6111.